NeuroImage 196 (2019) 227–236

Contents lists available at ScienceDirect

NeuroImage

journal homepage: www.elsevier.com/locate/neuroimage

Stimulus-response recoding during inhibitory control is associated with superior frontal and parahippocampal processes

Witold X. Chmielewski, Christian Beste *

Cognitive Neurophysiology, Department of Child and Adolescent Psychiatry, Faculty of Medicine of the TU Dresden, Germany

ARTICLE INFO

Keywords:
Theory of event coding
Event files
Response inhibition
EEG
sLORETA

ABSTRACT

Inhibitory control is affected by perceptual processes, but the mechanisms how perceptual features affect response inhibition are poorly understood. Theoretical frameworks detailing how variations in stimulus features that create overlaps between response categories can affect action control, like the Theory of Event Coding (TEC), have not been transferred to inhibitory control. We present a novel Go/Nogo paradigm in which we varied stimulus feature overlap between Go and Nogo trials. To examine what cognitive-neurophysiological subprocesses and functional neuroanatomical structures are modulated by stimulus-response feature overlap and recoding during inhibitory control, we combine event-related potential (ERP) recordings with source localization analyses. We show that response inhibition was compromised when stimulus features overlapped between Go and Nogo trials. The EEG data show that the recoding of stimulus-response mappings induced by such a stimulus feature overlaps affects subprocesses from perceptual gating/categorization (P1 ERP-component) to pre-motor inhibition (Nogo-N2 ERP-component) and motor inhibition (Nogo-P3 ERP-component). Although these are distinct processes, overlapping neuronal structures are associated with these modulations. The cascade of processes starts in the superior frontal cortex and is associated with perceptual categorization mechanisms. Subsequently, pre-motor inhibition or stimulus-response unbinding processes are modulated in parahippocampal structures before stimulus-response rebinding and motor inhibition is accomplished in parahippocampal and superior frontal structures. The study shows how perceptual processes can affect response inhibition using a theoretical framework, which has, until now, not been brought into connection with inhibitory control and establishes links between neurophysiology and functional neuroanatomy of inhibitory control with the TEC framework.

1. Introduction

Response inhibition processes are central for everyday life as they allow the inhibition of inappropriate behavior (Aron et al., 2014; Chambers et al., 2009; Diamond, 2013; Simmonds et al., 2008). There are various examples of cognitive measures of inhibitory control including tasks like Go/Nogo and Stop Signal tasks, as well as Simon and Flanker tasks (Diamond, 2013). Even though it is debated whether all of these tasks require inhibitory control (Diamond, 2013), some of these require intricate stimulus-response translation processes. The translation of sensory input to the motor output during response inhibition is of increasing interest, since modulations of early sensory and perceptual processes have repeatedly been shown to affect and predict response inhibition performance, e.g. in Go/Nogo tasks (Bodmer and Beste, 2017; Chmielewski et al., 2015; Chmielewski and Beste, 2016; Di Russo et al., 2016, 2006; Logan et al., 2014; Stock et al., 2016; Verbruggen et al., 2014).

One cognitive framework detailing how modulations of perceptual processes and stimulus features affect action control, and which may be suitable to address mechanisms of stimulus-response translation in the context of inhibitory control is the "Theory of event coding (TEC)" (Hommel et al., 2001). TEC assumes that the presentation of a stimulus requiring a specific response leads to a binding (i.e. an association between the stimulus and the response) (Hommel et al., 2001). These cognitive bindings between features constituting the stimulus and features constituting the response are established in so-called 'event files' (Hommel, 2015, 2009; Hommel et al., 2001). These, have also been described to resemble an episodic (memory) trace (Hommel, 2015, 2009). Within an event file, all stimuli and the associated actions are represented by their constituting features. This means that stimuli are

* Corresponding author. Cognitive Neurophysiology, Department of Child and Adolescent Psychiatry, TU Dresden, Germany, Schubertstrasse 42, D-01309, Dresden, Germany.
E-mail address: christian.beste@uniklinikum-dresden.de (C. Beste).

https://doi.org/10.1016/j.neuroimage.2019.04.035
Received 27 November 2018; Received in revised form 1 April 2019; Accepted 10 April 2019
Available online 13 April 2019

represented by features like stimulus color, shape, etc. Actions are also represented by their constituting features (e.g., which arm, hand, finger to use?). In an event file, bindings are established between each stimulus feature and each action (response) feature (Hommel, 1998), which why an event file is thought of to resemble a network of stimulus and response feature bindings. Therefore, processes in an event file and the activation of an event file follow a pattern completion logic (Hommel, 2009). An important consequence of this 'modus operandi' is that the entire event file can be (re-)activated once a single feature of a stimulus is (re-) encountered (Hommel, 2011): whenever there is a perception of even a single stimulus feature that has previously been integrated into an event file, this feature can activate the entire event file and trigger the associated/bound response (Hommel, 2005). Crucially, in cases where the same action has to be executed on the basis of a just slightly altered stimulus input, or when nearly identical stimulus input triggers opposing actions, previously established stimulus-response bindings cause problems (Colzato et al., 2006; Hommel, 2004). The reason is that the previously established stimulus-action-feature bindings are only partially fulfilled (Colzato et al., 2006; Hommel, 2004). Previously established expectations are therefore violated and interfere with the associations/bindings that need to be created upon the changed stimulus-response relationship. The consequence is that the event file has to be reconfigured. This event file reconfiguration is a time-consuming process, which slows behavior and makes it more error-prone. Such a decrease in behavioral efficacy as a consequence of event file reconfiguration and can be measured/index by so-called partial-repetition costs (Colzato et al., 2006; Hommel and Colzato, 2004). These are evident when comparing behavioral performance in trials with a full feature overlap with the standard stimulus-response mapping, compared to trials in which only some features of the stimulus-response mapping are included.

An important aspect why the TEC framework is very useful when being interested in the role of stimulus-response translation processes during response inhibition is that this framework is not only able to predict that a feature overlap between stimuli and response affects performance, but also *why* this is the case (Hommel, 2009). Notably, response inhibition is often conceptualized as a means to override automated response tendencies that develop across trials with consistent mappings of stimulus features on a response (no response) (Helton, 2009; Helton et al., 2005; Stevenson et al., 2011; Verbruggen and Logan, 2008). The impact of such 'automatically' created stimulus-response instances, or bindings have also been referred to as 'prepared reflex' and is a grounding principle of the TEC framework (Hommel, 2009). Moreover, an important principle of the TEC framework is that the framework draws no distinction between the execution and the inhibition of actions; i.e. both, the execution and the inhibition of responses are considered as 'action' (Hommel et al., 2001; Petruo et al., 2018). Intriguingly, also other evidence suggests that and inhibitory control processes are closely linked to action selection mechanisms (Bari and Robbins, 2013). This makes it reasonable to use the TEC-framework as a theoretical basis to examine stimulus-response translation processes in inhibitory control. This is also the case considering that neurobiological mechanisms show commonalities between event coding and response inhibition. For example, and similar to response inhibition processes (Bari and Robbins, 2013; Chambers et al., 2009), event coding is modulated by the dopaminergic system (Colzato et al., 2013, 2012; 2004; Colzato and Hommel, 2008; Petruo et al., 2016). Moreover, prefrontal regions like superior frontal areas including the supplemental motor area (SMA) and subcortical regions playing a role in response inhibition (Bari and Robbins, 2013; Beste et al., 2010; Chambers et al., 2009) have also been shown to be involved in event coding (Elsner et al., 2002; Kühn et al., 2011; Zmigrod et al., 2014).

Despite all this, essential principles of the TEC concept have not yet been transferred to response inhibition processes. They are, however, central to understand the role of perceptual processes during response inhibition and the role of stimulus-response recoding processes during inhibitory control. Until now, it is unknown which neurophysiological mechanisms and functional neuroanatomical structures are associated with such stimulus-response (event file) recoding or reconfiguration processes during inhibitory control. To close this gap, we designed a new response inhibition paradigm in which we varied the stimulus feature overlap between Go and Nogo trials (for details please refer to the methods section). Using EEG and source localization methods, we examined the effect of event file overlap during response inhibition at neurophysiological and functional neuroanatomical level.

Concerning behavioral performance, we hypothesized that a stimulus feature overlap between Go and Nogo stimuli are associated with partial repetition costs in inhibitory control. These costs are reflected by an increase in the false alarm rate (i.e. responses on Nogo trials) when Go and Nogo trials share stimulus features. Considering the EEG data, response inhibition subprocesses are reflected by the Nogo-N2 and Nogo-P3 event-related potentials (ERPs) (Huster et al., 2013). The Nogo- N2 is assumed to reflect pre-motor inhibition processes before intended movements (Beste et al., 2010; Falkenstein et al., 1999; Lavric et al., 2004; Smith et al., 2008). The Nogo-P3 is assumed to either reflect the inhibitory process itself, or an evaluation of the response inhibition process (Chmielewski and Beste, 2015; Falkenstein et al., 1999; Huster et al., 2011; Schmajuk et al., 2006; Wessel and Aron, 2015). As event file reconfiguration processes are time-consuming, we hypothesized that the Nogo-N2 and the Nogo-P3 latencies are longer when stimulus features overlap between Go and Nogo trials and compromise response inhibition performance. Using sLORETA we examined the functional neuroanatomical structures associated with these hypothesized effects. Previous results have shown that amplitude modulations of the Nogo-N2 and the Nogo-P3 are associated with activation differences in medial frontal, superior and inferior frontal areas (Huster et al., 2013). We, therefore, hypothesized that stimulus-response reconfiguration processes during inhibitory control modulate the Nogo-N2 and Nogo-P3, and this modulation is associated with activation differences in these areas. However, it needs to be considered that an event file reflects an episodic trace and reconfiguration processes therein have been suggested to involve parahippocampal areas (Hommel, 2009; Kühn et al., 2011). This seems reasonable because parahippocampal areas have otherwise been shown to process episodic traces and are assumed to process contextual associations (Aminoff et al., 2013), known to constitute event files (Hommel, 2009). Therefore, we hypothesized that aside prefrontal areas, parahippocampal regions are associated with modulations in neurophysiological processes underlying stimulus-response reconfiguration processes during inhibitory control. Indeed, there is tentative evidence that parahippocampal regions are involved in response inhibition, especially when contextual expectancies are violated (Chmielewski et al., 2016), or when inhibition errors are processed (Braet et al., 2011, 2009). However, the prerequisite of episodic memory trace reconfiguration is an appropriate categorization of stimulus information. The P1 ERP-component has been suggested to reflect this early categorization and gating of information into episodic traces (Freunberger et al., 2008; Klimesch, 2011; Klimesch et al., 2010) and has also been shown to be modulated during event file processing and reconfiguration (Petruo et al., 2016). Therefore, we hypothesized that aside classical ERP-correlates of inhibitory control (i.e. Nogo-N2 and Nogo-P3) the manipulation of stimulus-response reconfiguration processes during response inhibition modulates the P1 ERP-component. Since modulations of the P1 during inhibitory control tasks have already been shown to be associated with functional neuroanatomical structures in the response inhibition network (Giller et al., 2018; Wolff et al., 2018), we hypothesized that modulations of the P1 are also associated with these areas in the current study. This is all the more likely because prefrontal areas have been shown to play a major role in perceptual categorization processes (Freedman and Assad, 2016; McKee et al., 2014; Summerfield et al., 2011).

2. Materials and methods

2.1. Sample

We investigated N = 24 healthy participants (14 females; mean age 23.6 ± 0.7). EEG data from one participant had to be discarded due to poor data quality. The data analysis was thus run for N = 23 subjects. All participants gave written informed consent, were free of medication, did not report any neurological or psychiatric disorders and had normal or corrected-to-normal vision. The study was conducted in accordance with the declaration of Helsinki and was approved by the institutional review board of the Medical faculty of the TU Dresden. As outlined in the results, the power in the important interaction "Go/Nogo x even file overlap" and the power of the significant main effects ranged between $\eta_p^2 = 0.465$ and $\eta_p^2 = 0.274$, depending on the examined ERP-component. The obtained power in the study on N = 23 subjects was above 98%, which is due to the within-subject design used.

2.2. Task

We developed a 'TEC Go/Nogo' task in which Go and Nogo trials with or without stimulus feature overlap were presented. In this experiment, each trial started with the presentation of a stimulus for 450 ms. Trials lasted for 1700 ms, or unless they were terminated by the response. Trials were separated by an inter-trial interval (ITI), which was jittered between 800 and 1200 ms. Before the start of the experiment, a standardized training session with 30 trials was conducted to familiarize participants with the experiment. Participants were seated in a viewing distance of 56 cm vis-à-vis a 24'' TFT monitor, on which stimuli (4.2° visual angle) were presented on a black background in the center of the screen. Throughout the experiment, a fixation cross was presented in the center of the screen, except for the time points of stimulus presentation. In this experiment, Go stimuli (requiring a right-handed press of the space button) and Nogo stimuli (requiring no response) were presented. Go trials outweighed Nogo trials by approximately 70%–30% to induce prepotent response tendencies tempting participants to respond in Nogo trials (Dippel et al., 2016). To examine stimulus-response (event file) reconfiguration processes during response inhibition, Go and Nogo conditions were created with either overlapping or non-overlapping stimulus features. The conditions/stimuli of the task are shown in Fig. 1.

Non-overlapping event files for Go (N = 264 trials) and Nogo trials (N = 80 trials) were created by presenting the word 'PRESS' in green color in the Go condition, while the word 'STOPP' was presented in red color in the Nogo condition. In these Go and Nogo trials, the letter stimuli constituting the word, the color of these letter stimuli and the stimulus-response association were thus clearly distinct and should therefore not yield an overlapping event file structure. To create Go and Nogo trials with an overlap in their event file structure, stimulus features (i.e. letters and/or colours) overlapped between Go and Nogo trials. For these Go trials, either the word 'DRÜCK' was presented in white color (N = 264 trials), or the letters 'XXXXX' were presented in blue color (N = 264 trials). For the Nogo condition, either the word 'DRÜCK' was presented in blue color (N = 80 trials); or the letters 'XXXXX' were presented in white color (N = 80 trials) (refer to Fig. 1). Thus, considerable overlaps in stimulus features between Go and Nogo trials were evident. According to the pattern completion logic the presence of one stimulus feature, which is part of an event file, will automatically activate all features of this network (Hommel, 2011, 2009). This stimulus feature overlap between Go and Nogo event files makes it likely that Go event files are activated in Nogo conditions. This event file overlap should, therefore, lead to interferences, or partial repetition costs, which should induce an increased tendency to respond to Nogo stimuli. Overlapping Go and Nogo trials and non-overlapping Go and Nogo trials were pseudo-randomly presented in 8 equally-sized blocks. It was ensured that the frequency of overlapping and non-overlapping Go and Nogo trials was equal in each of these blocks. Between the blocks, the participants were allowed to a take a break.

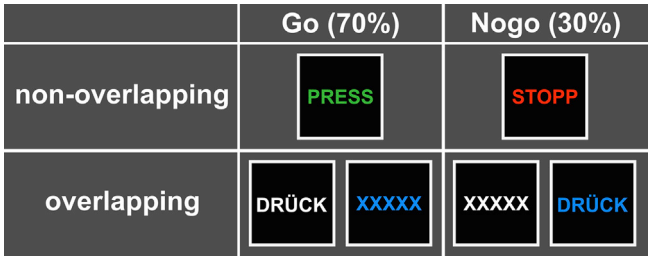

Fig. 1. Illustration of the different experimental Go and Nogo conditions used to induce overlaps in even files. For Go trials, either the word 'DRÜCK' was presented in white color, or the letters 'XXXXX' were presented in blue color. For the Nogo condition, either the word 'DRÜCK' was presented in blue color; or the letters 'XXXXX' were presented in white color (refer to Fig. 1). Thus, considerable overlaps in stimulus features between Go and Nogo trials were evident.

2.3. EEG recording and analysis

EEG data were recorded and analyzed with the Brain Vision Recorder/Analyzer 2 software (Brain Products Inc.). We used a sampling rate of 500 Hz and an electrode cap with 60 (Ag/AgCl) electrodes in equidistant positions to record our data. The reference electrode was positioned at the location Fpz and the ground electrode was positioned at coordinates θ = 58, ϕ = 78. For off-line data processing, we first applied a band-pass filter with a slope of 48db/oct to eliminate frequencies above 20 Hz and below 0.5 Hz. Additionally, a notch filter was used to eliminate residual frequencies at 50 Hz. Afterward, a manual raw data inspection was conducted to remove technical artifacts (e.g. offsets in the EEG). In the subsequent independent component analysis (ICA; infomax algorithm) recurring artifacts (e.g. pulse and vertical or horizontal eye movements) were detected and removed. In the following step, segments for the overlapping Go (including 'DRÜCK' in white and 'XXXXX' in blue) and Nogo condition (including 'DRÜCK' in blue and 'XXXXX' in white) and for the non-overlapping Go ('PRESS' in green) and Nogo condition ('STOPP' in red) was created. Segments started 250 ms prior to stimulus presentation and ended 1000 ms thereafter (segment length: 1250 ms). For these segments, an automated artifact rejection procedure was run, which discarded all segments with an activity smaller than 0.5 μV in a 100 ms time window, or in which the maximal amplitude exceeded ± 200 μV. This artifact rejection procedure eliminated N = 16 (±6) trials from the entire experiment in each subject. Thereafter, a current source density (CSD) transformation was conducted to obtain reference-free EEG data and to identify electrodes showing largest effects of the experimental modulations (Kayser and Tenke, 2015; Nunez and Pilgreen, 1991). The following specifications were used for the CSD transformation: A lambda approximation parameter of $1.00e^{-005}$, and an order of four splines and ten as the maximum degree for Legendre polynomials was used. Subsequently, we conducted a baseline correction in a time window of -200 – 0 ms prior to stimulus presentation. As the last step, we created averaged segments for all conditions at the single-subject level, i.e. for the overlapping Go, overlapping Nogo, non-overlapping Go and non-overlapping Nogo condition. By visual inspection of the scalp topography plots, we determined the electrodes and time windows for data quantification. To validate that the most important electrodes were chosen for data quantification, we used a statistical method described in Mückschel et al. (2014): During this procedure, the mean amplitude for every ERP-component in its respective time window at every single electrode is calculated. We then used Bonferroni-corrected multiple comparisons (employed threshold p = 0.007) to compare the single values extracted for each electrode to an average value of all other electrodes (except the compared electrode). Electrodes showing

significantly increased amplitudes in comparison to the average (positive for P1 & P3 and negative for N1 and N2) were selected. These electrodes were identical to the electrodes selected by means of the visual inspection. We quantified the following ERP-component amplitudes relative to baseline for every single subject: P1 (70–160 ms after stimulus presentation), N1 (120–230 ms after stimulus presentation). The peak of the P1 and N1 were quantified at electrodes P7 and P8. The N2 peak (225–375 ms after stimulus presentation) was quantified at electrode FCz and Cz. The P3 peak (300–600 ms after stimulus presentation) was quantified at electrodes Cz and Pz. These time windows and electrodes are usually analyzed in Go/Nogo paradigms (Huster et al., 2013). For a reliable peak quantification, it is mandatory that the different peaks are quantified at its maximum. **Based on the grand average waveforms, we took the peak amplitude latency of the condition showing the earliest peak and the peak amplitude latency of the longest peak as the boundary for the search interval. Because there may be differences between individuals, we added ± ~40 ms to that peak to estimate the search window for the peak detection algorithm.** As can be seen in Fig. 3, the peak latencies of the Nogo-P3 vary considerably between overlapping and non-overlapping Nogo trials, which is a hypothesized effect. Therefore, we verified whether the correct peak was identified by the automatic peak detection procedure. To do this, we visually inspected and double-checked each of the automatically quantified maxima to make sure that the correct peak was indeed identified by the automatic peak detection procedure. Only if this was clearly not the case (i.e. when the peak was outside the pre-specified time interval as outlined in the methods section), we corrected the marked time point accordingly so that it best depicted the peak of the Nogo-P3. Overall, this was only done in ~5% of cases. **The deviations only affected the N2 and P3 peaks (i.e. not the P1 and N1 peaks) and the mean deviation of the N2 and P3 peaks was 38 ± 10 ms across (N2: 32 ± 15 ms; P3: 45 ± 25 ms).** Using this data, the statistical analyses (ANOVAs) were run. However, to validate the effect, we re-run the data analysis using the mean amplitude value in the above-mentioned time windows to evaluate whether the same interaction effects are evident.

2.4. Source localization analyses

To localize sources that were associated with the P1, N1, N2, and P3 ERP-component modulations, we used sLORETA (standardized low-resolution brain electromagnetic tomography; Pascual-Marqui, 2002). The validity of sLORETA source estimations has been supported by combined fMRI/EEG and TMS/EEG studies (Dippel and Beste, 2015; Sekihara et al., 2005). sLORETA provides a single linear solution for the inverse issue, without localization bias (Marco-Pallarés et al., 2005; Pascual-Marqui, 2002; Sekihara et al., 2005). sLORETA is a properly standardized discrete, three-dimensional distributed, linear, minimum norm inverse solution. Extensive mathematical details can be found elsewhere (Pascual-Marqui, 2002). For sLORETA, the intra-cerebral volume is partitioned into 6239 voxels using a spatial resolution of 5 mm sLORETA uses a three-shell spherical head model and the covariance matrix was calculated using the single subject's baseline. Afterward, the standardized current density is calculated for every voxel, using an MNI152 head model template. For the identification sLORETA sources, we utilized voxel-wise randomization tests with 2500 permutations and statistical nonparametric mapping procedures (SnPM). The underlying rationale is (Nichols and Holmes, 2002) that if there is no experimental effect, the labeling of groups or conditions is arbitrary. Given that null hypothesis, the significance of a statistic expressing a significant effect is assessed by comparison with a distribution of values obtained when group/condition-memberships are permuted (Nichols and Holmes, 2002). Due to the non-parametric nature of the method, it does not require any assumption of Gaussianity. Locations of voxels that were significantly different ($p < .01$ using a correction for multiple comparisons) are shown in the MNI-brain www.unizh.ch/keyinst/NewLORETA/sLORETA/sLORETA.htm. Activations shown in the brain represent critical t-values corrected for multiple comparison. Since the overlapping Nogo trials are most important in the current study, this condition was focused in the sLORETA analyses. For the sLORETA procedure and the estimation of the sources, only the time windows used for ERP amplitude quantification were used.

2.5. Statistical analyses

Behavioral data were analyzed for Go and Nogo trials separately. Go hit rate and reaction time (RT) data, as well as Nogo false alarm (FA) data, were compared for conditions with overlapping vs. non-overlapping event files between Go and Nogo trials by means of post-hoc paired t-tests. For ERP-component latency and peak amplitude data, repeated measures ANOVAs including the within-subject factors "Go/Nogo (Go vs. Nogo)", "event file-overlap (overlapping vs. non-overlapping)" and "electrode" were conducted. Bonferroni-corrections for post-hoc testings and Greenhouse-Geisser corrections were used. As indicated by Kolmogorov-Smirnov Tests, all included variables were normally distributed (all $z < 0.8$; $p > .2$). For the descriptive statistics, the mean and standard error of the mean is given.

3. Results

3.1. Behavioral data

Concerning the Go accuracy data, paired t-tests revealed decreased hit rates in the overlapping (99.1 ± 0.2%) in comparison to the non-overlapping Go condition (99.6 ± 0.2%) ($t(22) = 3.72$; $p = .001$). For Go RTs, paired t-tests showed longer RTs in the overlapping (501 ± 12 ms) compared to the non-overlapping Go condition (479 ± 11 ms) ($t(22) = 4.70$; $p < .001$). Most importantly, for Nogo false alarm rates, paired t-tests showed that FAs were increased when Nogo stimulus features overlapped with Go stimulus features (27.7 ± 2.9%) in comparison to the conditions where no feature overlap of Go and Nogo stimuli was evident (0.7 ± 0.28%) ($t(22) = 9.70$; $p < .001$).

It is important to note that the two used stimuli for overlapping Go trials (i.e. 'DRÜCK' in white and 'XXXXX' in blue) and the two used stimuli for overlapping Nogo trials (i.e. 'DRÜCK' in blue and 'XXXXX' in white) did not differ from each other (all $p > .623$). The same was the case for the neurophysiological data in any of the ERP-components examined (all $p > .711$).

3.2. Neurophysiological data

As mentioned above, there were no differences in electrophysiological parameters between the two used stimuli for overlapping Go trials (i.e. 'DRÜCK' in white and 'XXXXX' in blue) and the two used stimuli for overlapping Nogo trials (i.e. 'DRÜCK' in blue and 'XXXXX' in white) (all $p > .711$). Below, all data and analyses are therefore presented pooled across these stimuli; i.e. 'DRÜCK' in white and 'XXXXX' in blue for overlapping Go trials and 'DRÜCK' in blue and 'XXXXX' in white for overlapping Nogo trials.

3.2.1. P1 ERP-component

The P1/N1 ERP-components are shown in Fig. 2.

There were no latency effects for the P1 and N1 ERP-components (all $F < 2.51$; $p > .109$). The repeated measures ANOVA for the P1 ERP-component amplitudes revealed a main effect of electrode ($F(1,22) = 6.68$; $p = .017$; $\eta_p^2 = 0.233$), showing decreased P1 amplitudes at P7 (31.3 ± 3.2 μV/m^2) in comparison to P8 (43.2 ± 4.6 μV/m^2). Moreover, a main effect of event file-overlap was detected ($F(1,22) = 7.05$; $p = .014$; $\eta_p^2 = 0.243$), showing decreased P1 amplitudes for overlapping (36.2 ± 3.3 μV/m^2) in comparison to non-overlapping conditions (38.4 ± 3.2 μV/m^2). Additionally, a main effect of Go/Nogo was detected ($F(1,22) = 11.32$; $p = .003$; $\eta_p^2 = 0.340$),

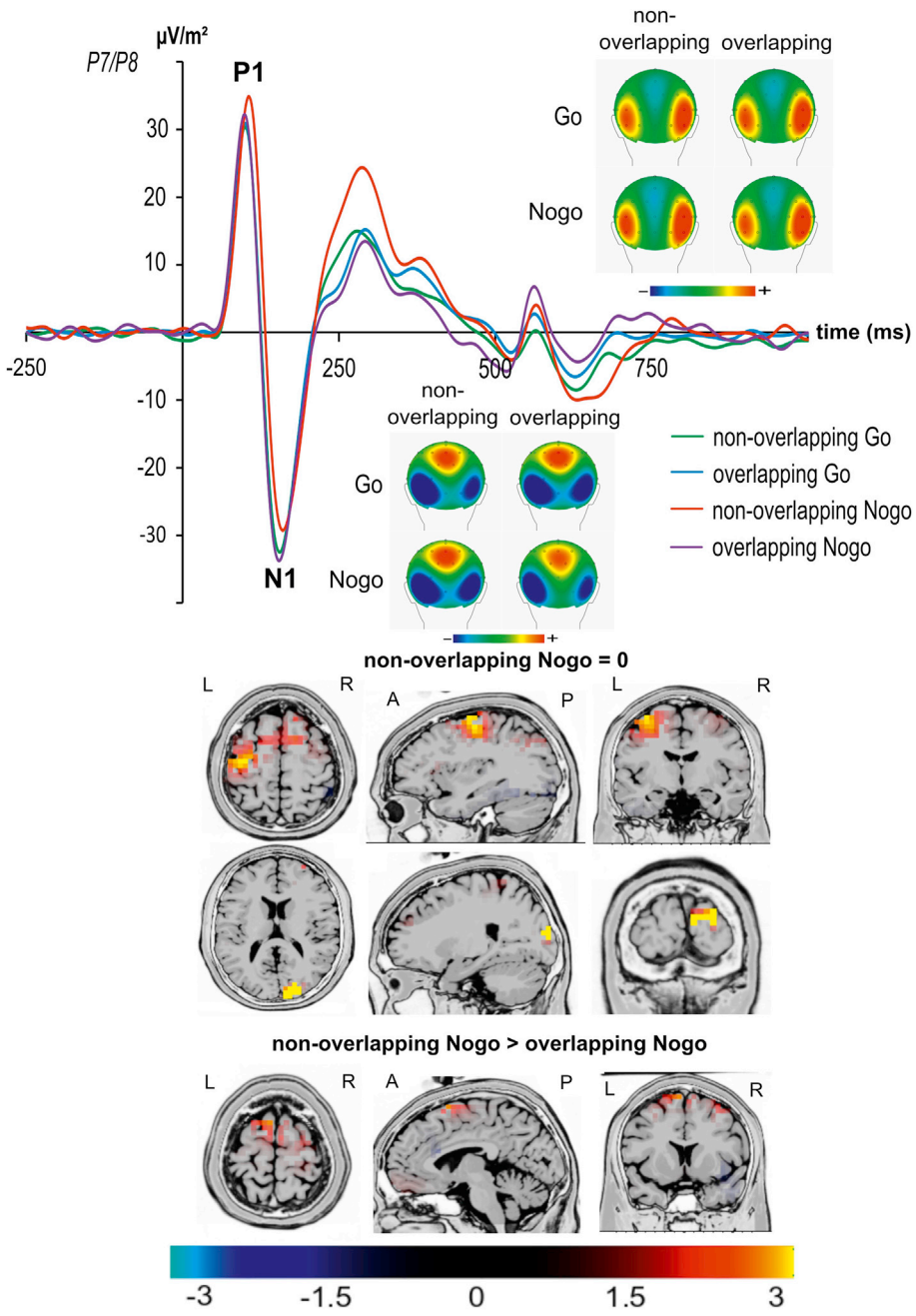

Fig. 2. The P1 and N1 ERP-components are shown, pooled across electrodes P7 and P8 including the scalp topography plots (red colours denote positive values, blue colours negative values). The scalp topography plots show the topography at the peak of the P1 and N1 components. The time point zero denotes the time point of stimulus presentation. The differences colours of the ERP time series denote the different experimental condition as outlined in the figure legend. The sLORETA plot (corrected for multiple comparisons using SnPM) shows the source of the P1 in the **non-**overlapping Nogo condition. A source in BA6 is delineated alongside with activation differences in the occipital cortex. A source in BA6 is also shown when comparing the overlapping and the non-overlapping condition with each other. The t-scores are lower (since the effect between conditions is smaller), but still significant even when correcting for multiple comparisons. For the sake of comparability, the same scale of critical t-values is shown for the contrast against zero and the contrast comparing the two experiment conditions against each other. In the sLORETA maps: A = anterior, P = posterior, L = left, R = right.

showing increased P1 amplitudes in Nogo ($38.7 \pm 3.4\,\mu V/m^2$) in comparison to Go ($35.8 \pm 3.1\,\mu V/m^2$) trials. Interestingly, an interaction Go/Nogo x event file-overlap was detected ($F(1,22) = 8.29$; $p = .009$; $\eta_p^2 = 0.274$), and this was also the case when the mean amplitude data was used for data analysis ($F(1,22) = 5.79$; $p = .025$; $\eta_p^2 = 0.232$). Additional interactions were not observed (all $F \leq 0.20$; $p \geq .663$).

Post-hoc paired t-tests tests using the peak amplitude data to examine the interaction Go/Nogo x event file-overlap revealed that this interaction was based on increased P1 amplitudes in the non-overlapping Nogo condition ($40.7 \pm 3.5\,\mu V/m^2$) in comparison to all other conditions, including the overlapping Nogo ($36.7 \pm 3.4\,\mu V/m^2$) condition (all $t \geq 3.34$; $p \leq .003$). The overlapping Go ($35.7 \pm 3.2\,\mu V/m^2$) and non-overlapping Go condition ($36.0 \pm 3.1\,\mu V/m^2$) did not significantly differ from each other (all $t \leq 1.23$; $p \geq .232$). The sLORETA analysis **revealed that the P1 amplitude in the non-overlapping Nogo condition** is associated with an activation in the superior frontal gyrus (BA6). It is shown that the 'activation maxima' were evident in BA6 (superior frontal gyrus) (MNI: 18, 1, 69), albeit in close relation to the middle frontal gyrus (BA6) (MNI: 23, 1, 69). This was also the case, when comparing the non-overlapping Nogo condition, with the overlapping condition BA6 (superior frontal gyrus) (MNI: 5, 9, 68). For that contrast, the t-scores are lower (since the effect between conditions is smaller), but still significant even when correcting for multiple comparisons. For the sake of comparability, the same scale of critical t-values is shown for the contrast against zero and the contrast comparing the two experiment conditions against each other. As can also be seen in Fig. 2, the P1 was associated with activation differences in the right middle occipital gyrus (BA18) (MNI: 23, −95, 14). This is mandatory finding in line with previous results on sources of the P1 (Herrmann and Knight, 2001). This activation was not evident when comparing the overlapping and the non-overlapping condition against each other, since the physical properties of the stimuli were not different between the conditions.

3.2.2. N1 ERP-component

In the repeated measures ANOVA for the N1 ERP-component amplitudes, an interaction electrode x event file-overlap was detected ($F(1,22) = 17.94$; $p < .001$; $\eta_p^2 = 0.340$). This interaction was due to significant differences between the overlapping ($-41.2 \pm 5.5\ \mu V/m^2$) and non-overlapping condition ($-34.6 \pm 4.7\ \mu V/m^2$) at electrode P8 ($t(22) = 3.92$; $p = .001$) but not at electrode P7 (overlapping: $39.0 \pm 4.7\ \mu V/m^2$; non-overlapping: $41.5 \pm 5.3\ \mu V/m^2$; $t(22) = -1.68$; $p = .108$). Yet, also a significant interaction Go/Nogo x event file-overlap was detected ($F(1,22) = 8.61$; $p = .008$; $\eta_p^2 = 0.281$) and the same interaction was found when using mean amplitude measures ($F(1,22) = 5.04$; $p = .035$; $\eta_p^2 = 0.199$). Post-hoc paired t-tests using the peak amplitude data revealed that this interaction was based on a significantly decreased N1 amplitude in the non-overlapping Nogo condition ($-36.1 \pm 4.3\ \mu V/m^2$) in comparison to all other conditions (all $t \geq 2.23$; $p \leq .036$), including the overlapping Nogo ($-40.5 \pm 4.5\ \mu V/m^2$) condition. The overlapping Go ($-39.6 \pm 4.5\ \mu V/m^2$) and non-overlapping Go condition ($-40.0 \pm 4.4\ \mu V/m^2$) did not significantly differ from each other ($t(22) = -0.48$; $p > .634$). The sLORETA analysis contrasting the overlapping Nogo to the non-overlapping Nogo condition revealed that these N1 amplitude modulations are associated with the cuneus (BA18) (maximal activity at MNI coordinates −23, −80, 18). Other main effects or interactions were not observed (all $F \leq 2.97$; $p \geq .099$). It is important to note that the differences in the N1 cannot reliably be interpreted since the preceding P1 peak was already different. Likely, this also affected the source of the N1.

3.2.3. N2 ERP-component

The N2 and P3 ERP-components are shown in Fig. 3.

In the repeated measures ANOVA for the N2 ERP-component (Fig. 3A) latencies the main effect of event file-overlap was observed ($F(1,22) = 13.62$; $p = .001$; $\eta_p^2 = 0.382$) showing N2 ERP-component latencies to be longer in overlapping (310 ± 5 ms) in comparison to non-overlapping conditions (289 ± 9 ms). More important, an interaction Go/Nogo x event file-overlap was observed ($F(1,22) = 19.17$; $p < .001$; $\eta_p^2 = 0.466$). While post-hoc tests showed that the overlapping (300 ± 7 ms) and non-overlapping Go (303 ± 9 ms) conditions did not differ from each other ($t = 0.82$; $p = .423$), there were latency differences for the overlapping and non-overlapping Nogo conditions ($t = 3.12$; $p = .005$). N2 latencies were longer in the overlapping Nogo condition (317 ± 10 ms), compared to the non-overlapping Nogo condition (278 ± 5 ms). For the critical overlapping Nogo condition, the sLORETA analysis (contrasting the overlapping Nogo condition to 0) revealed that the delayed N2 was associated with activation in the parahippocampal gyrus (BA30). Further details/discussions on the N2 source in the overlapping condition can be found in the supplemental material (i.e. Supplemental Fig. 1). **To examine whether the parahippocampal activation is specifically linked with the overlapping Nogo condition (and not with the non-overlapping No-Go condition), it is important to demonstrate that the sLORETA reveals BA30 activity that is significantly greater in the overlapping Nogo condition compared to the non-overlapping Nogo condition, in addition to the comparison against baseline. In fact, this is the case as shown in** Supplemental Fig. 2**.** In the repeated measures ANOVA for the N2 ERP-component amplitudes a main effect of Go/Nogo was observed ($F(1,22) = 6.93$; $p = .015$; $\eta_p^2 = 0.382$), showing that the N2 was larger in Nogo ($-17.0 \pm 2.7\ \mu V/m^2$), compared to Go trials ($-14.6 \pm 2.5\ \mu V/m^2$). Additionally, an interaction electrode x Go/Nogo x event file-overlap was detected ($F(1,22) = 4.99$; $p = .038$; $\eta_p^2 = 0.145$), but post-hoc tests did not withstand Bonferroni-correction (all $t \leq 1.17$; $p \geq .290$). The same main effect was found when using mean amplitude data observed ($F(1,22) = 4.93$; $p = .037$; $\eta_p^2 = 0.199$).

3.2.4. P3 ERP-component

The P3 ERP-component is shown in Fig. 3B. In the repeated measures ANOVA for P3 ERP-component latencies a main effect of electrode was detected ($F(1,22) = 17.48$; $p < .001$; $\eta_p^2 = 0.443$), showing longer P3 ERP-component latencies at electrode Cz (511 ± 11 ms) in comparison to Pz (418 ± 18 ms). Moreover, a main effect of event file-overlap was detected ($F(1,22) = 16.24$; $p = .001$; $\eta_p^2 = 0.425$), showing longer latencies in the overlapping (483 ± 11 ms) in comparison to non-overlapping (446 ± 11 ms) conditions. Additionally, the interactions "Go/Nogo x event file-overlap" ($F(1,22) = 18.22$; $p < .001$; $\eta_p^2 = 0.453$) and "electrode x Go/Nogo x event file-overlap" ($F(1,22) = 5.46$; $p = .029$; $\eta_p^2 = 0.199$) were significant. To examine the latter interaction in detail, repeated measures ANOVAs with the factors Go/Nogo and EF-overlap were conducted for the data from Pz and Cz electrodes separately: At electrode Pz an interaction Go/Nogo x EF-overlap was detected ($F(1,22) = 5.69$; $p = .026$; $\eta_p^2 = 0.205$). While post-hoc tests revealed no differences between the overlapping Go (416 ± 20 ms) and non-overlapping Go condition (413 ± 18 ms) ($t = 0.92$; $p = .339$), the latency was longer for the overlapping Nogo condition (446 ± 23 ms), compared to the non-overlapping Nogo condition (399 ± 19 ms) ($t = -4.88$; $p < .001$). The latency in the overlapping Nogo condition was also longer than in the Go conditions (all $t > 2.54$; $p < .013$). This interaction can therefore well explain the behavioral effects. For the overlapping Nogo condition, the sLORETA analysis (contrasting the overlapping Nogo condition to 0) revealed that the P3 ERP component was associated with an activation in the parahippocampal cortex (BA30) (maximal activity at MNI coordinates 16, -40, −5) and in the middle frontal gyrus (BA9) (maximal activity at MNI coordinates −44, 3, 40). For electrode Cz, an interaction Go/Nogo x EF-overlap was detected ($F(1,22) = 22.93$; $p < .001$; $\eta_p^2 = 0.510$). However, post-hoc tests revealed that the interaction at this electrode was driven by the non-overlapping Nogo condition, which differed from all other conditions (all $t \geq 3.86$; $p \leq .001$). The overlapping Nogo condition did not differ from the Go conditions (all $t \leq 1.29$; $p \geq .209$). Unlike the interaction at electrode Pz, the observed interaction at electrode Cz can therefore not explain the behavioral effects.

In the repeated measures ANOVA for P3 ERP-component amplitudes a main effect of electrode was detected ($F(1,22) = 7.11$; $p = .014$; $\eta_p^2 = 0.244$), showing smaller P3 amplitudes at Cz ($23.9 \pm 3.2\ \mu V/m^2$), compared to Pz ($33.2 \pm 3.0\ \mu V/m^2$). Moreover, a main effect of Go/Nogo was detected ($F(1,22) = 16.26$; $p = .001$; $\eta_p^2 = 0.425$), showing larger amplitudes in Nogo ($30.7 \pm 2.7\ \mu V/m^2$) than Go trials ($26.5 \pm 2.5\ \mu V/m^2$). An interaction Go/Nogo x event file-overlap was detected ($F(1,22) = 19.11$; $p < .001$; $\eta_p^2 = 0.465$), which was also significant when the mean amplitudes were used for data quantification ($F(1,22) = 6.29$; $p = .020$; $\eta_p^2 = 0.36$). Post-hoc paired t-tests showed this interaction to be related to increased P3 ERP-component amplitudes in the overlapping Nogo condition ($33.3 \pm 3.0\ \mu V/m^2$) in comparison to all other conditions (all $t \geq 3.45$; $p \leq .001$). The sLORETA analysis contrasting the overlapping Nogo condition with the non-overlapping Nogo condition revealed activation differences in the superior frontal gyrus (BA6) (maximal activity at MNI coordinates −20, −14, 69) and medial frontal gyrus (BA6) (maximal activity at MNI coordinates −5, −5, 62) (refer Fig. 3B). The non-overlapping Nogo condition did however not differ from both Go conditions (all $t \leq 1.54$; $p \geq .70$) and also the Go conditions did not differ from each other ($t(22) = 1.07$; $p = .125$).[1]

[1] Source localization estimates from the standard Go/Nogo trials can be found in the Supplemental Fig. 3 for the Nogo-N2 and Nogo-P3. These analyses show the canonical finding of activation differences in the anterior cingulate cortex (ACC) as well as the right inferior frontal gyrus. The obtained sources in the other conditions do therefore reflect specific effects of the experimental manipulation.

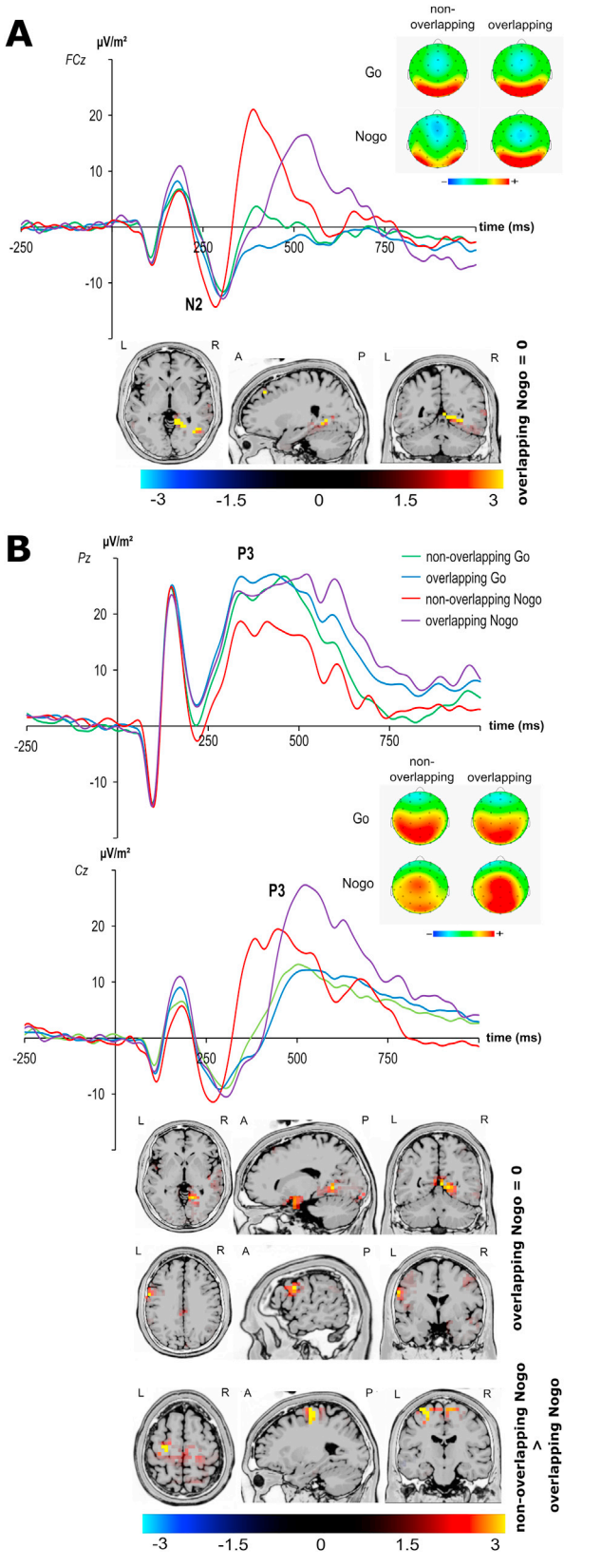

(caption on next column)

Fig. 3. (A) The N2 ERP-component is shown at electrode FCz including the scalp topography plots (red colours denote positive values, blue colours negative values). The scalp topography plots show the topography at the peak of the N2. The time point zero denotes the time point of stimulus presentation. The differences colours of the ERP time series denote the different experimental condition as outlined in the figure legend. The sLORETA plot (corrected for multiple comparisons using SnPM) shows the source of the Nogo-N2 in the overlapping condition. A source in the parahippocampal gyrus is delineated. Further information about the source of the Nogo-N2 in the overlapping condition can be found in the Supplemental Fig. 1. (B) The P3 ERP-component is shown at electrode Pz and Cz including the scalp topography plots (red colours denote positive values, blue colours negative values). The scalp topography plots show the topography at the peak of the P3. The time point zero denotes the time point of stimulus presentation. The differences colours of the ERP time series denote the different experimental condition as outlined in the figure legend. The sLORETA plot (corrected for multiple comparisons using SnPM) shows the source of the Nogo-3 in the overlapping condition. Moreover, the contrast "non-overlapping Nogo > overlapping Nogo" is shown. In the sLORETA maps: A = anterior, P = posterior, L = left, R = right.

4. Discussion

In the current study, we examined stimulus-response reconfiguration processes during inhibitory control using neurophysiological methods. This study was motivated by the fact that perceptual processes have a strong influence on response inhibition, but the influence of these processes has not yet been considered in relation to overarching theoretical concepts of action control. The goal of this study was to (i) show how perceptual processes can affect response inhibition using a theoretical framework, which has, until now, not been brought into connection with inhibitory control and (ii) to establish links between neurophysiology and functional neuroanatomy of inhibitory control with the TEC framework. We created a novel Go/Nogo task in which the stimulus feature overlap between Go and Nogo trials was varied. We used the TEC framework because this framework is not only able to predict that a feature overlap between stimuli and response affects performance, but also *why* this is the case. Other theories on inhibitory control like the dual mechanisms of control frame work (Braver, 2012), accounts on unexpected events (Wessel and Aron, 2017), as well as functional neuroanatomical network or modular perspective on inhibitory control (Hampshire and Sharp, 2015), do not make explicit assumptions why and how stimulus-response feature overlaps may impact inhibitory control. It has been pointed out that 'holistic approaches' are needed to understand different instances of cognitive control (Hampshire and Sharp, 2015). TEC clearly represents such a holistic approach.

The behavioral data are well in line with the hypothesis that a stimulus feature overlap between Go and Nogo trials compromises response inhibition processes. The rate of false alarms was higher, when stimulus features were part of Go and Nogo trials, compared to conditions in which Go and Nogo trials did not share stimulus features. Even though the effects of overlapping event files were also evident in RTs and hit rates during Go trials, the effects were smaller than in Nogo trials. The specific ratio of Go and Nogo trials (i.e. 70% vs. 30%) has been shown to induce a rather 'automated' response tendency (Dippel et al., 2016; Helton, 2009; Helton et al., 2005; McVay and Kane, 2009; Quetscher et al., 2015; Stevenson et al., 2011), imposing high demands on response inhibition processes (Dippel et al., 2017, 2016; Dockree et al., 2006, 2004). Thus, the results suggest that the effect of event file reconfiguration processes scales with the demands on cognitive control processes and that this effect not that much evident when cognitive control processes are less demanded during rather 'automated' response execution.

The neurophysiological data suggest that a multitude of processes and functional neuroanatomical structures are involved in stimulus-response reconfiguration processes during inhibitory control. The same interaction effects were obtained using peak amplitudes and mean amplitudes in

particular time window, which underlines the reliability of the obtained results. In line with our expectations, interactions of "Go/Nogo x event file-overlap" were already evident for the P1 ERP-component and the source localization suggested that the superior frontal gyrus (SFG, BA6) is associated with these modulations. The SFG is part of the response inhibition network (Bari and Robbins, 2013). During inhibitory control tasks, previous data have shown that modulations of the P1 originate from prefrontal brain regions that have also been implicated in the cortical response inhibition network (Giller et al., 2018; Wolff et al., 2018). The current data show that the P1 and activity in BA6 were reduced in overlapping, compared to non-overlapping Nogo conditions; i.e. the P1 and BA6 activity was reduced in that Nogo condition which also revealed an increased rate of false alarms. Several lines of evidence suggest that the P1 reflects inhibitory gating and categorization mechanisms which control the access of incoming information to task sets/representations and episodic traces (Klimesch, 2011; Klimesch et al., 2010). Other data suggested that successful reconfiguration of overlapping event files is associated with increased P1 amplitudes (Petruo et al., 2016). The pattern may therefore be interpreted that inhibitory gating in trials presenting stimuli with a high feature overlap between Go and Nogo trials is harder than in trials presenting stimuli with no feature overlap between Go and Nogo trials. This is also in line with the poorer behavioral performance in the overlapping Nogo trials. Thus, a critical aspect during stimulus-response reconfiguration processes in inhibitory control is how easy early gating and categorization processes can be deployed. It is possible that BA6 is associated with these processes in the current study because this region plays an essential role in inhibitory control (Bari and Robbins, 2013). Yet, lateral and superior frontal regions have otherwise been shown to be involved in perceptual categorization (Freedman and Assad, 2016; Smith and Grossman, 2008). The increased N1 amplitudes in the overlapping, compared to the non-overlapping Nogo condition likely reflect increased attentional processing (Herrmann and Knight, 2001), which may be necessary to fully evaluate the ambiguous stimulus features in the overlapping Nogo condition.

Concerning response control, the data revealed that the latency of the Nogo-N2 was prolonged in the overlapping Nogo condition. The sLORETA analysis revealed a source in parahippocampal gyrus (BA30) for the Nogo-N2 in the overlapping Nogo condition (contrast: overlapping Nogo > 0). The shift of the Nogo-N2 peak latency is in line with our expectations. As outlined, event file reconfiguration (i.e. unbinding and rebinding) processes are likely necessary when stimulus-response associations overlap between Go and Nogo trials. Since these processes are time-consuming, it makes ample sense that the Nogo-N2 latency is prolonged. Interestingly, it has been suggested that the Nogo-N2 reflects *premotor* inhibitory control processes (Huster et al., 2013); i.e. a revision of a motor plan/program before the actual motor process (Beste et al., 2010; Falkenstein et al., 1999). As mentioned, the event file contains a network of bindings between all features specifying a stimulus and all features specifying the motor response (Hommel, 1998). Reconfiguration of an event file requires that these bindings need to be adjusted or revised. Also, other data has already shown that processes in the N2 time window are associated with the reconfiguration or unbinding of elements in the event file (Petruo et al., 2016) and the retrieval of this episodic file (Spapé et al., 2011). Against the background that modulations in the N2 time window are associated with the retrieval of the episodic trace during response selection (Spapé et al., 2011) it seems reasonable that the parahippocampal gyrus is associated with these processes (Aminoff et al., 2013). In most studies on response inhibition the N2 is, however, not associated with the parahippocampal area, but almost exclusively with prefrontal brain areas (Huster et al., 2013). Yet, these studies do not vary the feature overlap between Go and Nogo stimuli and do thus not require reconfigurations of episodic traces specifying stimulus-response relationships. Rather, they use clearly distinct stimulus categories to trigger responding or response inhibition. The contribution of the parahippocampal gyrus in the current study therefore likely results from the relatively intricate unbinding and reconfiguration processes of event file traces as induced by a stimulus feature overlap.

Opposed to the N2 time window, processes in the P3 time window have been suggested to reflect the rebinding of an event file in the sense of the implementation of an action (Petruo et al., 2016). In line with that, the Nogo-P3 has been suggested to reflect the implementation of motor inhibition process per se (Beste et al., 2016; Dutra et al., 2018; Huster et al., 2013; Wessel and Aron, 2015). A natural prerequisite for such an implementation of action is that elements in the event file are rebound (Hommel, 2009). The data show that the Nogo-P3 peak latency was longer in the overlapping than in the non-overlapping condition. The amplitude of the Nogo-P3 was also larger in the overlapping, compared to the non-overlapping condition. This pattern can be interpreted that it takes longer for motor inhibition processes to become fully effective if there are overlaps in stimulus features leading to less distinct Go and Nogo event files. The higher Nogo-P3 amplitudes in the overlapping Nogo condition further suggest that motor inhibition processes need to be intensified. The sLORETA analysis showed that the parahippocampal regions and the superior frontal cortex (BA6) were activated. The interpretation of intensified motor inhibition processes associated with BA6 is well in line with other findings from lesion studies suggesting that the superior and medial frontal (pre-)supplementary motor area (Allen et al., 2018; Chen et al., 2009; Floden and Stuss, 2006; Sumner et al., 2007) as well as the premotor cortex (Hung et al., 2018; Sharp et al., 2010) are important to allow a successful inhibition of a motor response. The intensified motor inhibition processes in the case of the overlapping Nogo condition are likely a consequence of the overlapping stimulus features between Go and Nogo trials. The integration of a Go feature into a Nogo stimulus leads to an increased response tendency, which is then only partly controlled by intensified inhibition processes. This leads to a strengthened and delayed neuronal response (i.e. Nogo-P3). The involvement of parahippocampal cortices during the modulation of the Nogo-P3 can be explained by the fact that during re-binding aspects of the event file are changed. Since this is a modification of an episodic trace, it seems plausible that parahippocampal structures are involved that are known to play a significant role in such processes (Aminoff et al., 2013).

In summary, the study examined the neurophysiological and functional neuroanatomical correlates of stimulus-response reconfiguration processes during inhibitory control. The data show that conceptual principles of TEC can be applied to response inhibition processes and predict the effects of modulations at the perceptual level on the efficacy to inhibit a response. The EEG data show that stimulus-response recoding during inhibitory control affects various temporally and functionally distinct subprocesses from perceptual gating and categorization processes (P1 ERP-component) to pre-motor inhibition (Nogo-N2 ERP-component) and motor inhibition processes (Nogo-P3 ERP-component). These distinct subprocesses depend on partially overlapping functional neuroanatomical structures. The observed cascade of neurophysiological subprocesses starts in the superior frontal cortex which is associated with perceptual categorization mechanisms. Subsequently, pre-motor inhibition or event file unbinding processes in parahippocampal structures are modulated before event file rebinding and motor inhibition again associated with parahippocampal and superior frontal structures is accomplished.

Acknowledgments

This work was supported by a Grant from the Deutsche Forschungsgemeinschaft FOR 2698.

Appendix A. Supplementary data

Supplementary data to this article can be found online at https://doi.org/10.1016/j.neuroimage.2019.04.035.

References

Allen, C., Singh, K.D., Verbruggen, F., Chambers, C.D., 2018. Evidence for parallel activation of the pre-supplementary motor area and inferior frontal cortex during response inhibition: a combined MEG and TMS study. Roy. Soc. Open Sci. 5, 171369. https://doi.org/10.1098/rsos.171369.

Aminoff, E.M., Kveraga, K., Bar, M., 2013. The role of the parahippocampal cortex in cognition. Trends Cognit. Sci. 17, 379–390. https://doi.org/10.1016/j.tics.2013.06.009.

Aron, A.R., Robbins, T.W., Poldrack, R.A., 2014. Inhibition and the right inferior frontal cortex: one decade on. Trends Cognit. Sci. 18, 177–185. https://doi.org/10.1016/j.tics.2013.12.003.

Bari, A., Robbins, T.W., 2013. Inhibition and impulsivity: behavioral and neural basis of response control. Prog. Neurobiol. 108, 44–79. https://doi.org/10.1016/j.pneurobio.2013.06.005.

Beste, C., Stock, A.-K., Epplen, J.T., Arning, L., 2016. Dissociable electrophysiological subprocesses during response inhibition are differentially modulated by dopamine D1 and D2 receptors. Eur. Neuropsychopharmacol. J. Eur. Coll. Neuropsychopharmacol. 26, 1029–1036. https://doi.org/10.1016/j.euroneuro.2016.03.002.

Beste, C., Willemssen, R., Saft, C., Falkenstein, M., 2010. Response inhibition subprocesses and dopaminergic pathways: basal ganglia disease effects. Neuropsychologia 48, 366–373. https://doi.org/10.1016/j.neuropsychologia.2009.09.023.

Bodmer, B., Beste, C., 2017. On the dependence of response inhibition processes on sensory modality. Hum. Brain Mapp. 38, 1941–1951. https://doi.org/10.1002/hbm.23495.

Braet, W., Johnson, K.A., Tobin, C.T., Acheson, R., Bellgrove, M.A., Robertson, I.H., Garavan, H., 2009. Functional developmental changes underlying response inhibition and error-detection processes. Neuropsychologia 47, 3143–3151. https://doi.org/10.1016/j.neuropsychologia.2009.07.018.

Braet, W., Johnson, K.A., Tobin, C.T., Acheson, R., McDonnell, C., Hawi, Z., Barry, E., Mulligan, A., Gill, M., Bellgrove, M.A., Robertson, I.H., Garavan, H., 2011. fMRI activation during response inhibition and error processing: the role of the DAT1 gene in typically developing adolescents and those diagnosed with ADHD. Neuropsychologia 49, 1641–1650. https://doi.org/10.1016/j.neuropsychologia.2011.01.001.

Braver, T.S., 2012. The variable nature of cognitive control: a dual mechanisms framework. Trends Cognit. Sci. 16, 106–113. https://doi.org/10.1016/j.tics.2011.12.010.

Chambers, C.D., Garavan, H., Bellgrove, M.A., 2009. Insights into the neural basis of response inhibition from cognitive and clinical neuroscience. Neurosci. Biobehav. Rev. 33, 631–646. https://doi.org/10.1016/j.neubiorev.2008.08.016.

Chen, C.-Y., Muggleton, N.G., Tzeng, O.J.L., Hung, D.L., Juan, C.-H., 2009. Control of prepotent responses by the superior medial frontal cortex. Neuroimage 44, 537–545. https://doi.org/10.1016/j.neuroimage.2008.09.005.

Chmielewski, W.X., Beste, C., 2016. Perceptual conflict during sensorimotor integration processes - a neurophysiological study in response inhibition. Sci. Rep. 6, 26289. https://doi.org/10.1038/srep26289.

Chmielewski, W.X., Beste, C., 2015. Action control processes in autism spectrum disorder – insights from a neurobiological and neuroanatomical perspective. Prog. Neurobiol. 124, 49–83. https://doi.org/10.1016/j.pneurobio.2014.11.002.

Chmielewski, W.X., Mückschel, M., Stock, A.-K., Beste, C., 2015. The impact of mental workload on inhibitory control subprocesses. Neuroimage 112, 96–104. https://doi.org/10.1016/j.neuroimage.2015.02.060.

Chmielewski, W.X., Wolff, N., Mückschel, M., Roessner, V., Beste, C., 2016. Effects of multisensory integration processes on response inhibition in adolescent autism spectrum disorder. Psychol. Med. 46, 2705–2716. https://doi.org/10.1017/S0033291716001008.

Colzato, L.S., Erasmus, V., Hommel, B., 2004. Moderate alcohol consumption in humans impairs feature binding in visual perception but not across perception and action. Neurosci. Lett. 360, 103–105. https://doi.org/10.1016/j.neulet.2004.01.054.

Colzato, L.S., Hommel, B., 2008. Cannabis, cocaine, and visuomotor integration: evidence for a role of dopamine D1 receptors in binding perception and action. Neuropsychologia 46, 1570–1575. https://doi.org/10.1016/j.neuropsychologia.2007.12.014.

Colzato, L.S., van Wouwe, N.C., Hommel, B., Zmigrod, S., Ridderinkhof, K.R., Wylie, S.A., 2012. Dopaminergic modulation of the updating of stimulus-response episodes in Parkinson's disease. Behav. Brain Res. 228, 82–86. https://doi.org/10.1016/j.bbr.2011.11.034.

Colzato, L.S., Warrens, M.J., Hommel, B., 2006. Priming and binding in and across perception and action: a correlational analysis of the internal structure of event files. Q. J. Exp. Psychol. 59, 1785–1804. https://doi.org/10.1080/17470210500438304.

Colzato, L.S., Zmigrod, S., Hommel, B., 2013. Dopamine, norepinephrine, and the management of sensorimotor bindings: individual differences in updating of stimulus-response episodes are predicted by DAT1, but not DBH5'-ins/del. Exp. Brain Res. 228, 213–220. https://doi.org/10.1007/s00221-013-3553-x.

Di Russo, F., Lucci, G., Sulpizio, V., Berchicci, M., Spinelli, D., Pitzalis, S., Galati, G., 2016. Spatiotemporal brain mapping during preparation, perception, and action. Neuroimage 126, 1–14. https://doi.org/10.1016/j.neuroimage.2015.11.036.

Di Russo, F., Taddei, F., Apnile, T., Spinelli, D., 2006. Neural correlates of fast stimulus discrimination and response selection in top-level fencers. Neurosci. Lett. 408, 113–118. https://doi.org/10.1016/j.neulet.2006.08.085.

Diamond, A., 2013. Executive functions. Annu. Rev. Psychol. 64, 135–168. https://doi.org/10.1146/annurev-psych-113011-143750.

Dippel, G., Beste, C., 2015. A causal role of the right inferior frontal cortex in implementing strategies for multi-component behaviour. Nat. Commun. 6, 6587. https://doi.org/10.1038/ncomms7587.

Dippel, G., Chmielewski, W., Mückschel, M., Beste, C., 2016. Response mode-dependent differences in neurofunctional networks during response inhibition: an EEG-beamforming study. Brain Struct. Funct. 221, 4091–4101. https://doi.org/10.1007/s00429-015-1148-y.

Dippel, G., Mückschel, M., Ziemssen, T., Beste, C., 2017. Demands on response inhibition processes determine modulations of theta band activity in superior frontal areas and correlations with pupillometry - implications for the norepinephrine system during inhibitory control. Neuroimage 157, 575–585. https://doi.org/10.1016/j.neuroimage.2017.06.037.

Dockree, P.M., Bellgrove, M.A., O'Keeffe, F.M., Moloney, P., Aimola, L., Carton, S., Robertson, I.H., 2006. Sustained attention in traumatic brain injury (TBI) and healthy controls: enhanced sensitivity with dual-task load. Exp. Brain Res. 168, 218–229. https://doi.org/10.1007/s00221-005-0079-x.

Dockree, P.M., Kelly, S.P., Roche, R.A.P., Hogan, M.J., Reilly, R.B., Robertson, I.H., 2004. Behavioural and physiological impairments of sustained attention after traumatic brain injury. Brain Res. Cogn. Brain Res. 20, 403–414. https://doi.org/10.1016/j.cogbrainres.2004.03.019.

Dutra, I.C., Waller, D.A., Wessel, J.R., 2018. Perceptual surprise improves action stopping by nonselectively suppressing motor activity via a neural mechanism for motor inhibition. J. Neurosci. Off. J. Soc. Neurosci. 38, 1482–1492. https://doi.org/10.1523/JNEUROSCI.3091-17.2017.

Elsner, B., Hommel, B., Mentschel, C., Drzezga, A., Prinz, W., Conrad, B., Siebner, H., 2002. Linking actions and their perceivable consequences in the human brain. Neuroimage 17, 364–372.

Falkenstein, M., Hoormann, J., Hohnsbein, J., 1999. ERP components in Go/Nogo tasks and their relation to inhibition. Acta Psychol. 101, 267–291. https://doi.org/10.1016/S0001-6918(99)00008-6.

Floden, D., Stuss, D.T., 2006. Inhibitory control is slowed in patients with right superior medial frontal damage. J. Cogn. Neurosci. 18, 1843–1849. https://doi.org/10.1162/jocn.2006.18.11.1843.

Freedman, D.J., Assad, J.A., 2016. Neuronal mechanisms of visual categorization: an abstract view on decision making. Annu. Rev. Neurosci. 39, 129–147. https://doi.org/10.1146/annurev-neuro-071714-033919.

Freunberger, R., Höller, Y., Griesmayr, B., Gruber, W., Sauseng, P., Klimesch, W., 2008. Functional similarities between the P1 component and alpha oscillations. Eur. J. Neurosci. 27, 2330–2340. https://doi.org/10.1111/j.1460-9568.2008.06190.x.

Giller, F., Zhang, R., Roessner, V., Beste, C., 2019. The neurophysiological basis of developmental changes during sequential cognitive flexibility between adolescents and adults. Hum. Brain Mapp. 40, 552–565. https://doi.org/10.1002/hbm.24394.

Hampshire, A., Sharp, D.J., 2015. Contrasting network and modular perspectives on inhibitory control. Trends Cognit. Sci. 19, 445–452. https://doi.org/10.1016/j.tics.2015.06.006.

Helton, W.S., 2009. Impulsive responding and the sustained attention to response task. J. Clin. Exp. Neuropsychol. 31, 39–47. https://doi.org/10.1080/13803390801978856.

Helton, W.S., Hollander, T.D., Warm, J.S., Matthews, G., Dember, W.N., Wallaart, M., Beauchamp, G., Parasuraman, R., Hancock, P.A., 2005. Signal regularity and the mindlessness model of vigilance. Br. J. Psychol. Lond. Engl. 1953 (96), 249–261. https://doi.org/10.1348/000712605X38369.

Herrmann, C.S., Knight, R.T., 2001. Mechanisms of human attention: event-related potentials and oscillations. Neurosci. Biobehav. Rev. 25, 465–476.

Hommel, B., 2015. The theory of event coding (TEC) as embodied-cognition framework. Front. Psychol. 6, 1318. https://doi.org/10.3389/fpsyg.2015.01318.

Hommel, B., 2011. The Simon effect as tool and heuristic. Acta Psychol. 136, 189–202. https://doi.org/10.1016/j.actpsy.2010.04.011.

Hommel, B., 2009. Action control according to TEC (theory of event coding). Psychol. Res. 73, 512–526. https://doi.org/10.1007/s00426-009-0234-2.

Hommel, B., 2005. How much attention does an event file need? J. Exp. Psychol. Hum. Percept. Perform. 31, 1067–1082. https://doi.org/10.1037/0096-1523.31.5.1067.

Hommel, B., 2004. Event files: feature binding in and across perception and action. Trends Cognit. Sci. 8, 494–500. https://doi.org/10.1016/j.tics.2004.08.007.

Hommel, B., 1998. Event files: evidence for automatic integration of stimulus-response episodes. Vis. Cognit. 5. https://doi.org/10.1080/713756773.

Hommel, B., Colzato, L., 2004. Visual attention and the temporal dynamics of feature integration. Vis. Cognit. 11, 483–521. https://doi.org/10.1080/13506280344000400.

Hommel, B., Müsseler, J., Aschersleben, G., Prinz, W., 2001. The Theory of Event Coding (TEC): a framework for perception and action planning. Behav. Brain Sci. 24, 849–878. https://doi.org/10.1017/S0140525X01000103.

Hung, Y., Gaillard, S.L., Yarmak, P., Arsalidou, M., 2018. Dissociations of cognitive inhibition, response inhibition, and emotional interference: voxelwise ALE meta-analyses of fMRI studies. Hum. Brain Mapp. 39, 4065–4082. https://doi.org/10.1002/hbm.24232.

Huster, R.J., Eichele, T., Enriquez-Geppert, S., Wollbrink, A., Kugel, H., Konrad, C., Pantev, C., 2011. Multimodal imaging of functional networks and event-related potentials in performance monitoring. Neuroimage 56, 1588–1597. https://doi.org/10.1016/j.neuroimage.2011.03.039.

Huster, R.J., Enriquez-Geppert, S., Lavallee, C.F., Falkenstein, M., Herrmann, C.S., 2013. Electroencephalography of response inhibition tasks: functional networks and cognitive contributions. Int. J. Psychophysiol. Off. J. Int. Organ. Psychophysiol. 87, 217–233. https://doi.org/10.1016/j.ijpsycho.2012.08.001.

Kayser, J., Tenke, C.E., 2015. On the benefits of using surface Laplacian (current source density) methodology in electrophysiology. Int. J. Psychophysiol. Off. J. Int. Organ. Psychophysiol. 97, 171–173. https://doi.org/10.1016/j.ijpsycho.2015.06.001.

Klimesch, W., 2011. Evoked alpha and early access to the knowledge system: the P1 inhibition timing hypothesis. Brain Res. 1408, 52–71. https://doi.org/10.1016/j.brainres.2011.06.003.

Klimesch, W., Freunberger, R., Sauseng, P., 2010. Oscillatory mechanisms of process binding in memory. Neurosci. Biobehav. Rev. 34, 1002–1014. https://doi.org/10.1016/j.neubiorev.2009.10.004.

Kühn, S., Keizer, A.W., Colzato, L.S., Rombouts, S.A.R.B., Hommel, B., 2011. The neural underpinnings of event-file management: evidence for stimulus-induced activation of and competition among stimulus-response bindings. J. Cogn. Neurosci. 23, 896–904. https://doi.org/10.1162/jocn.2010.21485.

Lavric, A., Pizzagalli, D.A., Forstmeier, S., 2004. When 'go' and 'nogo' are equally frequent: ERP components and cortical tomography. Eur. J. Neurosci. 20, 2483–2488. https://doi.org/10.1111/j.1460-9568.2004.03683.x.

Logan, G.D., Van Zandt, T., Verbruggen, F., Wagenmakers, E.-J., 2014. On the ability to inhibit thought and action: general and special theories of an act of control. Psychol. Rev. 121, 66–95. https://doi.org/10.1037/a0035230.

Marco-Pallarés, J., Grau, C., Ruffini, G., 2005. Combined ICA-LORETA analysis of mismatch negativity. Neuroimage 25, 471–477. https://doi.org/10.1016/j.neuroimage.2004.11.028.

McKee, J.L., Riesenhuber, M., Miller, E.K., Freedman, D.J., 2014. Task dependence of visual and category representations in prefrontal and inferior temporal cortices. J. Neurosci. Off. J. Soc. Neurosci. 34, 16065–16075. https://doi.org/10.1523/JNEUROSCI.1660-14.2014.

McVay, J.C., Kane, M.J., 2009. Conducting the train of thought: working memory capacity, goal neglect, and mind wandering in an executive-control task. J. Exp. Psychol. Learn. Mem. Cogn. 35, 196–204. https://doi.org/10.1037/a0014104.

Mückschel, M., Stock, A.-K., Beste, C., 2014. Psychophysiological mechanisms of interindividual differences in goal activation modes during action cascading. Cerebr. Cortex 24, 2120–2129. https://doi.org/10.1093/cercor/bht066.

Nichols, T.E., Holmes, A.P., 2002. Nonparametric permutation tests for functional neuroimaging: a primer with examples. Hum. Brain Mapp. 15, 1–25. https://doi.org/10.1002/hbm.1058.

Nunez, P.L., Pilgreen, K.L., 1991. The spline-Laplacian in clinical neurophysiology: a method to improve EEG spatial resolution. J. Clin. Neurophysiol. Off. Publ. Am. Electroencephalogr. Soc. 8, 397–413.

Pascual-Marqui, R.D., 2002. Standardized low-resolution brain electromagnetic tomography (sLORETA): technical details. Methods Find. Exp. Clin. Pharmacol. 24 (Suppl. D), 5–12.

Petruo, V., Bodmer, B., Brandt, V.C., Baumung, L., Roessner, V., Münchau, A., Beste, C., 2018. Altered perception-action binding modulates inhibitory control in Gilles de la Tourette syndrome. JCPP (J. Child Psychol. Psychiatry). https://doi.org/10.1111/jcpp.12938.

Petruo, V.A., Stock, A.-K., Münchau, A., Beste, C., 2016. A systems neurophysiology approach to voluntary event coding. Neuroimage 135, 324–332. https://doi.org/10.1016/j.neuroimage.2016.05.007.

Quetscher, C., Yildiz, A., Dharmadhikari, S., Glaubitz, B., Schmidt-Wilcke, T., Dydak, U., Beste, C., 2015. Striatal GABA-MRS predicts response inhibition performance and its cortical electrophysiological correlates. Brain Struct. Funct. 220, 3555–3564. https://doi.org/10.1007/s00429-014-0873-y.

Schmajuk, M., Liotti, M., Busse, L., Woldorff, M.G., 2006. Electrophysiological activity underlying inhibitory control processes in normal adults. Neuropsychologia 44, 384–395. https://doi.org/10.1016/j.neuropsychologia.2005.06.005.

Sekihara, K., Sahani, M., Nagarajan, S.S., 2005. Localization bias and spatial resolution of adaptive and non-adaptive spatial filters for MEG source reconstruction. Neuroimage 25, 1056–1067. https://doi.org/10.1016/j.neuroimage.2004.11.051.

Sharp, D.J., Bonnelle, V., De Boissezon, X., Beckmann, C.F., James, S.G., Patel, M.C., Mehta, M.A., 2010. Distinct frontal systems for response inhibition, attentional capture, and error processing. Proc. Natl. Acad. Sci. U. S. A 107, 6106–6111. https://doi.org/10.1073/pnas.1000175107.

Simmonds, D.J., Pekar, J.J., Mostofsky, S.H., 2008. Meta-analysis of Go/No-go tasks demonstrating that fMRI activation associated with response inhibition is task-dependent. Neuropsychologia 46, 224–232. https://doi.org/10.1016/j.neuropsychologia.2007.07.015.

Smith, E.E., Grossman, M., 2008. Multiple systems of category learning. Neurosci. Biobehav. Rev. 32, 249–264. https://doi.org/10.1016/j.neubiorev.2007.07.009.

Smith, J.L., Johnstone, S.J., Barry, R.J., 2008. Movement-related potentials in the Go/NoGo task: the P3 reflects both cognitive and motor inhibition. Clin. Neurophysiol. 119, 704–714. https://doi.org/10.1016/j.clinph.2007.11.042.

Spapé, M.M., Band, G.P.H., Hommel, B., 2011. Compatibility-sequence effects in the Simon task reflect episodic retrieval but not conflict adaptation: evidence from LRP and N2. Biol. Psychol. 88, 116–123. https://doi.org/10.1016/j.biopsycho.2011.07.001.

Stevenson, H., Russell, P.N., Helton, W.S., 2011. Search asymmetry, sustained attention, and response inhibition. Brain Cogn. 77, 215–222. https://doi.org/10.1016/j.bandc.2011.08.007.

Stock, A.-K., Popescu, F., Neuhaus, A.H., Beste, C., 2016. Single-subject prediction of response inhibition behavior by event-related potentials. J. Neurophysiol. 115, 1252–1262. https://doi.org/10.1152/jn.00969.2015.

Summerfield, C., Behrens, T.E., Koechlin, E., 2011. Perceptual classification in a rapidly changing environment. Neuron 71, 725–736. https://doi.org/10.1016/j.neuron.2011.06.022.

Sumner, P., Nachev, P., Morris, P., Peters, A.M., Jackson, S.R., Kennard, C., Husain, M., 2007. Human medial frontal cortex mediates unconscious inhibition of voluntary action. Neuron 54, 697–711. https://doi.org/10.1016/j.neuron.2007.05.016.

Verbruggen, F., Logan, G.D., 2008. Automatic and controlled response inhibition: associative learning in the go/no-go and stop-signal paradigms. J. Exp. Psychol. Gen. 137, 649–672. https://doi.org/10.1037/a0013170.

Verbruggen, F., Stevens, T., Chambers, C.D., 2014. Proactive and reactive stopping when distracted: an attentional account. J. Exp. Psychol. Hum. Percept. Perform. 40, 1295–1300. https://doi.org/10.1037/a0036542.

Wessel, J.R., Aron, A.R., 2017. On the globality of motor suppression: unexpected events and their influence on behavior and cognition. Neuron 93, 259–280. https://doi.org/10.1016/j.neuron.2016.12.013.

Wessel, J.R., Aron, A.R., 2015. It's not too late: the onset of the frontocentral P3 indexes successful response inhibition in the stop-signal paradigm. Psychophysiology 52, 472–480. https://doi.org/10.1111/psyp.12374.

Wolff, N., Giller, F., Buse, J., Roessner, V., Beste, C., 2018. When repetitive mental sets increase cognitive flexibility in adolescent obsessive-compulsive disorder. JCPP (J. Child Psychol. Psychiatry) 59, 1024–1032. https://doi.org/10.1111/jcpp.12901.

Zmigrod, S., Colzato, L.S., Hommel, B., 2014. Evidence for a role of the right dorsolateral prefrontal cortex in controlling stimulus-response integration: a transcranial direct current stimulation (tDCS) study. Brain Stimul. 7, 516–520. https://doi.org/10.1016/j.brs.2014.03.004.